

# Precise Image Unwarping for Omnidirectional Cameras with Hyperbolic-Shaped Mirrors

Sheng-Wen Jeng (鄭勝文) and Wen-Hsiang Tsai (蔡文祥)

Department of Computer & Information Science

National Chiao Tung University

1001 Ta Hsueh Rd., Hsinchu, Taiwan 300, R. O. C.

e-mails: sunny@ccl.itri.org.tw, whtsai@cis.nctu.edu.tw

Tels: 886-3-5914557, 886-3-5712121 Ext. 31751

## Abstract

Unwarping an omnidirectional image into a perspective-view image is easy for the single-viewpoint (SVP) designed catadioptric omnidirectional camera. But misalignment between the components (such as the mirror and the lens) of this kind of camera leads to multiple viewpoints and distorts the unwrapped image if the SVP constraint is still assumed. We release the SVP constraint for unwarping images taken from an omnidirectional camera with a hyperbolic-shaped mirror (called a hypercatadioptric camera below) by using the internal calibration information to derive new image unwarping equations. It is found that by reducing the calibration parameters to fit the SVP constraint, the resulting unwrapped images are almost of no difference from that of the ideal SVP method. We have so extended the unwarping ability of the hypercatadioptric camera to tolerate camera integration errors, which is useful for many application purposes.

## Keywords:

Omnidirectional camera, single viewpoint (SVP), unwarping, hypercatadioptric camera, camera calibration.

## 1. Introduction

It is well known in computer vision that increasing the field of view (FOV) enhances the visual coverage, reduces dead corners, and saves the computation time of a vision system, especially in applications such as visual surveillance and robot navigation.

There are many ways to design a camera system consisting of lens/mirrors and CCD sensors to increase the FOV for a vision system [1]. An extreme way to expand the FOV to the full hemisphere is to use a catadioptric system, which is an integration of a convex reflection mirror, an orthographic (or perspective) projection lens, and a CCD sensor chip. A popular name for this kind of design is *omnidirectional camera*. Depending on the design, the surface curve of the reflection mirror can be conical, spherical, parabolic, or hyperbolic, and

the lens can be of the type of orthographic or perspective projection. To simplify the unwarping process of omnidirectional images to normal perspective ones, a catadioptric omnidirectional camera is usually designed to fit the “single-viewpoint” (or “single center-of-projection”) constraint. In the above mirror/lens combinations, only the combination of the parabolic mirror and the orthographic lens or that of the hyperbolic mirror and the perspective lens can fit the “single-viewpoint” constraint. If the single-viewpoint constraint is not met, the locus of viewpoints forms what is called a “caustic” curve [2], and in such a case, the unwarping work is very complicated. When the parabolic mirror is used, we call it a “paracatadioptric” camera, and when the hyperbolic mirror is used, we will call it a “hypercatadioptric” camera, following the idea of [7]. In this study, we deal with the image unwarping problem for the hypercatadioptric camera.

In this paper, we use the *internal calibrated parameters* to derive the precise mapping equations for the hypercatadioptric camera, which is not a single-viewpoint system. Here, the internal calibrated parameters include the pose of the camera with respect to the mirror (also called mirror/camera misalignment, which includes center-to-center translation and plane-to-plane rotation) as well as the camera intrinsic parameters.

The calibration method used here is Tsai’s single-view coplanar method [5], and the calibration pattern is a thin-ring with 16 black-bar-marks equally distributing over the ring border. The inner diameter of the ring is equal to the bottom diameter of the hyperbolic mirror. The calibration pattern is attached at the border of the mirror, where the marks are projected visually directly onto the image plane. After the calibration work, the basic optical reflection law as well as the co-planar constraints of the mirror surface normal, the incident ray, and the reflected ray are applied to derive a set of mapping equations between a pixel in the image coordinate system and a point in the world space. The calibrated camera parameters are used as known parameters in these derived mapping equations. Using the derived mapping equations, we can unwrap precisely an omnidirectional image taken by the

hypercatadioptric camera into an image from any perspective view (for example, from the top view or the side view).

This paper deals with precise unwarping problems of the non-SVP designed hypercatadioptric camera. Our contribution is deriving a set of unwarping equations using the combination of a simple calibration method and the basic optical image-formation rules. These equations are general forms of image mapping between an image point and a world point for the hypercatadioptric camera. With these set of equations, unwarping omni-image of the hypercatadioptric camera to a perspective-view image is not confined to the SVP designed type only.

The remainder of this paper is organized as follows. In Section 2, we review the basic concepts about single-viewpoint omnidirectional cameras and some previous works for omnidirectional camera calibration. The camera calibration method proposed in this paper is described in Section 3. In Section 4, the procedures of deriving the unwarping formulas using the calibrated data are described in detail. In Section 5, some experimental results with simulation data and real images are given. Finally, we make some conclusions in Section 6.

## 2. Review of Previous Works

For an ideal single-viewpoint omnidirectional camera using the parabolic mirror/orthographic lens combination (i.e., for a paracatadioptric camera), the relation between a point in space  $(x_p, y_p, z_p)$  and its projected image point  $(x_i, y_i)$  on the image plane is as follows [1] (see Fig. 1 for the definitions of the symbols):

$$x_i = \rho \sin \theta \cos \phi, \quad y_i = \rho \sin \theta \sin \phi \quad (1)$$

where

$$\theta = \cos^{-1} \frac{z_p}{\sqrt{x_p^2 + y_p^2 + z_p^2}}, \quad \phi = \tan^{-1} \frac{y_p}{x_p} \quad (2)$$

and

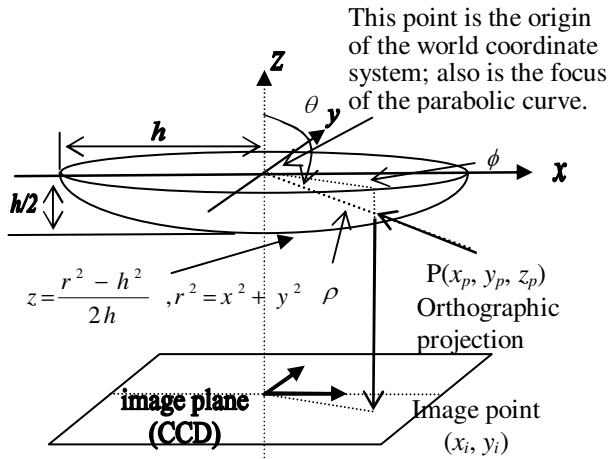


Fig. 1 A paracatadioptric camera with orthographic projection.

$$\rho = \frac{h}{1 + \cos \theta} \quad \text{for } \frac{\pi}{2} < \theta < \pi. \quad (3)$$

Or combining the above equations, we get

$$x_i = \frac{hx_p}{\sqrt{x_p^2 + y_p^2 + z_p^2 + z_p}}, \quad y_i = \frac{hy_p}{\sqrt{x_p^2 + y_p^2 + z_p^2 + z_p}}. \quad (4)$$

For an ideal single-viewpoint omnidirectional camera using the hyperbolic mirror/perspective lens combination (i.e., for a hypercatadioptric camera), the relation between a point in space  $(x_p, y_p, z_p)$  and its projected image point  $(x_i, y_i)$  on the image plane is as follows [3, 4] (see Fig. 2 for the definitions of the symbols):

$$x_i = \frac{f(b^2 - c^2)x_p}{(b^2 + c^2)z_p - 2bc\sqrt{x_p^2 + y_p^2 + z_p^2}}, \quad (5)$$

$$y_i = \frac{f(b^2 - c^2)y_p}{(b^2 + c^2)z_p - 2bc\sqrt{x_p^2 + y_p^2 + z_p^2}}$$

where  $c = \sqrt{a^2 + b^2}$ .

Equation (4) or (5) represents the mapping between a point  $(x_i, y_i)$  in the image plane and its corresponding world point  $(x_p, y_p, z_p)$  under perfect single-viewpoint design and known system parameters. The known system

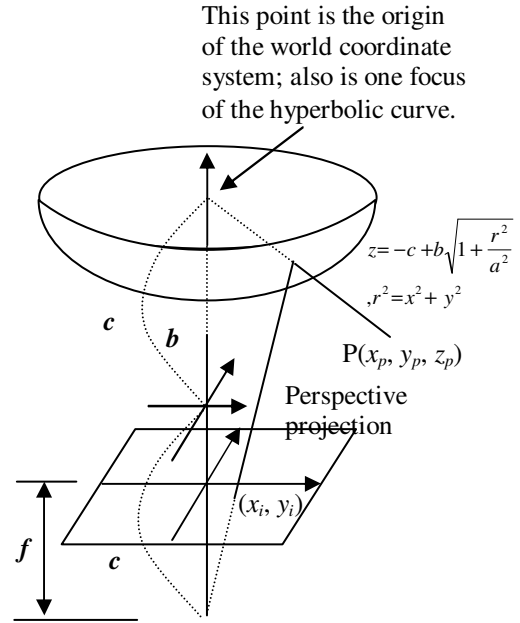


Fig. 2 A hypercatadioptric camera with perspective projection.

parameters include the focal length of a parabolic mirror  $h/2$  in Fig. 1 or the focal length  $f$  and the mirror curve parameters  $a$ ,  $b$  and  $c$  in Fig. 2. In practical conditions, the point  $(x_i, y_i)$  may be shifted from the expected position caused by the lens distortion, and the mirror center may be misaligned to the center of the camera coordinate system. So, the final position of the point  $(x_i, y_i)$

in the image coordinate system (which is stored at computer memory) is:

$$\begin{aligned} u_i &= s_x [x_i (1 + \kappa_1 r^2 + \kappa_2 r^4)] + C_x, \\ v_i &= s_y [y_i (1 + \kappa_1 r^2 + \kappa_2 r^4)] + C_y \end{aligned} \quad (6)$$

where  $r = \sqrt{x_i^2 + y_i^2}$ ,  $s_x, s_y$  are the scaling factors for the  $x$  and  $y$  directions when mapping from the camera coordinate to the image coordinate,  $(C_x, C_y)$  is the projected point of the mirror center on the image coordinate system, and  $\kappa_1$  and  $\kappa_2$  are the radial distortion factors of the lens [5, 6].

In a conventional perspective camera system, which includes only a lens and a CCD sensor, the parameters in Equation (6) and the focal length  $f$  are called ‘‘intrinsic’’ parameters. The intrinsic parameters also exist in the omnidirectional camera system. To estimate the intrinsic parameters, the calibration procedure should be done before conducting accurate measurement or 3D reconstruction in a conventional perspective camera system or unwarping omnidirectional images into perspective-view images in a catadioptric omnidirectional camera system. In [7, 8], Geyer proposed closed-form solutions for the focal length, the image (mirror) center, and the aspect ratio (these are intrinsic parameters) to calibrate a paracatadioptric camera using a single view of three lines. In [9], Kang used the consistency condition of pair-wise tracked point features across a sequence of paracatadioptric images to calibrate the same parameters in [7, 8]. Basically, in [7, 8, 9] they dealt with the ideal SVP paracatadioptric camera, so the integration errors between the mirror and the lens/CCD sensor (here we call this combination as ‘‘camera’’ in the following paragraphs) were not considered (here, the  $x$ - $y$  plane of the camera coordinate system was assumed parallel to the  $x$ - $y$  plane of the mirror coordinate system). Only the intrinsic parameters of the cameras were taken into account. So, Equation (4) was still be used to unwarped the omnidirectional image to a perspective image, except that the image point  $(x_i, y_i)$  should be modified using the derived equations in their papers similar to the concept in Equation (6). The quality of the unwarped image in [7, 8, 9] is strongly depend on the slipping degrees from the SVP design of their paracatadioptric camera, although the intrinsic parameters of their cameras had been calibrated.

If the SVP constraints can not be preserved for a catadioptric omnidirectional camera due to the integration errors between the mirror and the camera or the non-SVP design is adopted for the reason to increase the FOV [2], beside the intrinsic parameters of the camera need to be calibrated, the pose of the mirror related to the camera needs to be calibrated too. In [10], Aliaga developed a calibration model using a beacon-based pose estimation algorithm for the non-SVP catadioptric omnidirectional camera which is designed using the combination of a

parabolic mirror and a perspective lens (Note that this kind of mirror/lens combination is surely 100% non-SVP design!). Aliaga’s camera model, like Tsai’s [5], has eleven parameters (5 intrinsic and 6 extrinsic). But, the physical meanings of the extrinsic parameters are different from those of Tsai’s, with the translation vector  $(t_x, t_y, t_z)$  representing the offset between the mirror reference plane and the image plane (CCD sensor plane), the rotation vector  $(r_x, r_y, r_z)$  representing the rotation of the mirror reference plane with respect to an assumed world coordinate frame (a position of beacon). In Aliaga’s paper, the rotation angle of the mirror reference plane with respect to the CCD sensor plane was implicitly assumed to be zero. The calibrated data were used to estimate the pose of the catadioptric camera in a room-size environment. In this case, unwarping image was not necessary. In fact, it is very difficult to get the unwarped image in this kind of catadioptric camera.

A more complete calibration procedure for a catadioptric camera which estimates the intrinsic camera parameters and the pose of the mirror related to the camera appeared at [11]. In [11], Fabrizio used the images of two known radius circles at two different planes in an omnidirectional camera structure to calibrate the intrinsic camera parameters and the camera pose with respect to the mirror. But, in [11], no discussion was made about how to use the calibrated parameters to modify the mapping Equations (4) or (5) for getting an accurate unwarped perspective image from an omnidirectional image.

In this study, we deal with the unwarping problems caused by the non-SVP designed hypercatadioptric camera. We propose a simple calibration idea to get all the needed information of the hypercatadioptric camera using Tsai’s [5] calibration method. The calibrated data are used to derive a set of mapping equations between an image point and its corresponding incident line in the world. Then, the derived equations are applied to unwarped the omnidirectional image to any defined type of perspective image. We prove in this paper that this set of equations is a powerful tool to deal with any kinds of hypercatadioptric camera.

### 3. Camera Calibration

#### 3.1 Structure of Hypercatadioptric Camera

The structure of a hyperbolic-shaped omnidirectional (hypercatadioptric) camera is depicted in Fig. 3. The surface curve of the hyperbolic mirror is defined under the world coordinate system,  $b$  is the distance from the origin  $W$  to the tip of the mirror,  $h$  is the height of the mirror (at the center), and  $m$  is the radius of the mirror bottom.

A point  $M(x_m, y_m, z_m)$  on the mirror surface with respect to the origin  $W$  of the world coordinate system can be described by the following equations

according to the 3D geometry of the hypercatadioptric camera:

$$z_m = b \sqrt{1 + \frac{r_m^2}{a^2}}, \quad r_m^2 = x_m^2 + y_m^2. \quad (7)$$

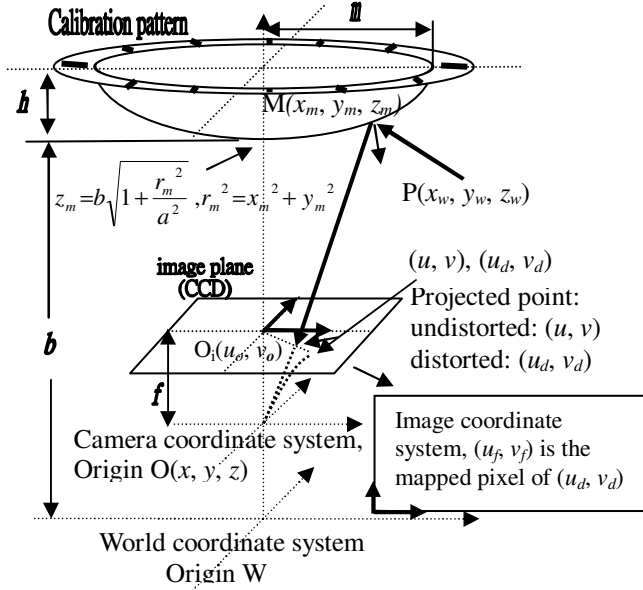


Fig 3. The structure of a hyperbolic-shaped omnidirectional (hypercatadioptric) camera.

The optical center  $O(x, y, z)$  is defined as the origin of the 3D camera coordinate system, and the optical axis is aligned with the  $z$ -axis of the world coordinate system. The projection point of the optical axis on the image (CCD sensor) plane ( $z = f$ ) of the camera coordinate system is  $O_i(u_o, v_o)$  which is also the center of the image plane. We set  $(u_o, v_o) = (0, 0)$ .

The mirror parameters  $a, b, h$ , and  $m$ , and the physical size of the CCD sensor, are obtained from the specifications of the hypercatadioptric camera.

### 3.2 Details of Proposed Calibration Work

#### 3.2.1 Proposed calibration pattern

In this study, we draw a *calibration pattern* on a paper ring and attach it on the mirror mount around the mirror border for use in the calibration work. The shape of the calibration pattern consists of an inner circle with a diameter equal to that of the mirror as well as 16 black marks of small line segments evenly distributed around the circle border. An example image of the attached pattern is showed in Fig. 4. It is noted that only 12 marks are visible in the FOV.

Because the calibration pattern is located outside the reflection mirror, it is projected onto the image plane directly. The short-bar marks lay on the same  $x$ - $y$  plane (at known  $z$  value) of the world coordinate system. Each inner tip coordinate  $(x_w, y_w, z_w)$  of the mark relative to the origin  $W$  of the world coordinate can be describe as follows:

$$x_{wi} = m \times \cos(i \times \theta),$$

$$y_{wi} = m \times \sin(i \times \theta), \quad i = 0, 1, 2, \dots, 15, \quad \theta = 22.5^\circ$$

$$z_{wi} = b + h$$



Fig.4 An image of the calibration pattern.

#### 3.2.2 Coordinate systems for calibration

Fig. 5 depicts the coordinate systems and the definition of parameters used in this paper for the calibration work. In this paper, we first get the relation between the calibration coordinate and the camera coordinate, than we transfer the relation to the camera coordinate and the world coordinte, which represents the pose of the camera with respect to the mirror. Here, we assume the lens and the CCD sensor plane (image plane) are perfect aligned. So, a point on the  $z$ -axis of the camera coordinate system is projected at the center of the CCD sensor, which is located at the center pixel  $(C_x, C_y)$  on the image coordinate (computer buffer).

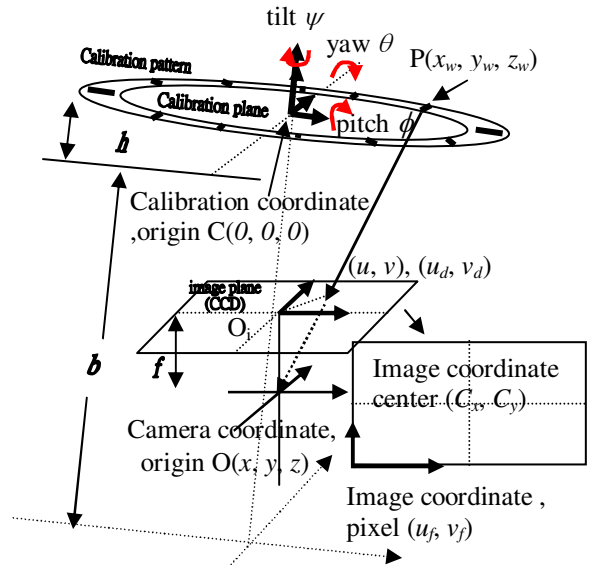


Fig. 5 Coordinate systems for calibration.

A point  $P(x_w, y_w, z_w)$  of the calibration pattern on the calibration plane can be expressed relative to the origin of the camera coordinate system as

Equation (8). Where, R is a 3x3 rotation matrix with three rotation angles around the x-axis (pitch  $\phi$ ), y-axis (yaw  $\theta$ ) and z-axis (tilt  $\psi$ ) of the calibration coordinate system respectively. (remark: In the book "Computer and Robot Vision" by Robert M. Haralick,  $\phi$  is called as tilt,  $\theta$  is called as pan and  $\psi$  is called as swing) Here, rotation follows by translation operation is adopted.

$$\begin{bmatrix} x \\ y \\ z \end{bmatrix} = R \begin{bmatrix} x_w \\ y_w \\ z_w \end{bmatrix} + T \quad (8)$$

where

$$R = \begin{bmatrix} \cos \Psi \cos \theta & \sin \Psi \cos \theta & -\sin \theta \\ -\sin \Psi \cos \phi + \cos \Psi \sin \theta \sin \phi & \cos \Psi \cos \phi + \sin \Psi \sin \theta \sin \phi & \cos \theta \sin \phi \\ \sin \Psi \sin \phi + \cos \Psi \sin \theta \cos \phi & -\cos \Psi \sin \phi + \sin \Psi \sin \theta \cos \phi & \cos \theta \cos \phi \end{bmatrix} \quad (8-1)$$

$$\text{or } R = \begin{bmatrix} r_{11} & r_{12} & r_{13} \\ r_{21} & r_{22} & r_{23} \\ r_{31} & r_{32} & r_{33} \end{bmatrix}$$

is the rotation matrix, where  $r_{11} = \cos \Psi \cos \theta$ ,  $r_{12} = \sin \Psi \cos \theta$ , ...etc.

$$\text{and } T = \begin{bmatrix} T_x \\ T_y \\ T_z \end{bmatrix} \text{ is the translation vector.}$$

The projected point  $(u, v)$  of  $P(x, y, z)$  on the image plane (CCD sensor) is as follow:

$$u = f \frac{x}{z}, \quad v = f \frac{y}{z} \quad (\text{perspective projection}) \quad (9)$$

When the lens distortion (only the radial direction) is considered, the following relations should be taken into account.

$$u_d + D_x = u, \quad v_d + D_y = v \quad (\text{radial lens distortion})$$

where:

$$D_x = \kappa_1 u_d r^2, \quad D_y = \kappa_1 v_d r^2, \quad r^2 = u_d^2 + v_d^2$$

or

$$u = u_d (1 + \kappa_1 r^2), \quad v = v_d (1 + \kappa_1 r^2) \quad (10)$$

The pixel coordinate in computer buffer is as follow:

$$u_f = S_x u_d + C_x, \quad v_f = S_y v_d + C_y \quad (11)$$

### 3.2.3 Calculating the calibration parameters

The known calibration points  $(x_{wi}, y_{wi}, z_{wi})$  on the calibration plane and their projected points in the image coordinate system  $(u_{fi}, v_{fi})$ ,  $i=0,1..n$ , can be used to solve Equations (8) to (11). The entire  $z_{wi}$  equal zeros, because they are located on the calibration plane. In this paper, the points  $(u_{fi}, v_{fi})$ ,  $i=0,1..n$ , are obtained manually by using mouse to click the locations in the calibration image like as Fig. 4.

Using Tsai's single view coplanar calibration

method [5] and assuming that the parameter  $f$  is known from the data sheet. We get the calibration parameters R, T and  $\kappa_1$ , which are the *internal calibrated parameters* mentioned in Section 1.

### 3.2.4 Deriving the pose of the camera with respect to the mirror

The rotation matrix R and the translation vector T derived in section 3.2.3 is the pose of the calibration plane with respect to the camera. In this paper, for deriving the modified mapping formulas of Equation (5), we should transfer the coordinates to get the pose of the camera with respect to the mirror. In this paper, the origin of the mirror coordinate system is defined at a focus point of the hyperbolic mirror curve ( $O_m$  at Fig. 6). The camera origin  $O$  is related to the mirror origin  $O_m$  by Equation (12). Assume its coordinate is  $(x_{cw}, y_{cw}, z_{cw})$  in the mirror coordinate system.

$$\begin{aligned} x_{cw} &= -T_x, \\ y_{cw} &= -T_y, \end{aligned} \quad (12)$$

$$z_{cw} = -T_z + (b + h) - c$$

The coordinate of a point  $I$  in the camera coordinate system is  $(u, v, f)$ . So, the point  $I$  in the mirror coordinate system is:

$$\begin{aligned} u_i &= ur'_{11} + vr'_{12} + fr'_{13} - T_x, \\ v_i &= ur'_{21} + vr'_{22} + fr'_{23} - T_y, \end{aligned} \quad (13)$$

$$z_i = ur'_{31} + vr'_{32} + fr'_{33} - T_z + (b + h) - c$$

$$\text{Where, the new rotation matrix } R' = \begin{bmatrix} r'_{11} & r'_{12} & r'_{13} \\ r'_{21} & r'_{22} & r'_{23} \\ r'_{31} & r'_{32} & r'_{33} \end{bmatrix}$$

is obtained by reverse the signs of  $(\phi, \theta, \psi)$  in Equation (8-1), which is  $(\phi_c, \theta_c, \psi_c)$ .

## 4. Back-Projection of Image Point

From Section 3, the correct camera model for image formation is depicted as Fig.6. In Fig.6, the angle of pitch  $\phi_c$ , yaw  $\theta_c$  and tilt  $\psi_c$  are the negative values of the calibrated rotation angle of pitch  $\phi$ , yaw  $\theta$  and tilt  $\psi$  in Fig. 5. When the pose of the camera with respect to the mirror is determined at section 3.2.4 after calibration, the unit vector  $(w_x, w_y, w_z)$  of the incident ray on the mirror surface point  $M(x_m, y_m, z_m)$  can be uniquely determined by a point  $(u, v)$  at the image plane. In the following paragraphs, all the formulas derived are based on the mirror coordinate system.

Two constraints are used in this paper to derive the relation between  $(w_x, w_y, w_z)$  and  $(u, v)$ .

- (1) The surface normal  $\vec{n}$  and points  $P, M, O$  are co-planar.
- (2) The reflection law of mirror should be held.

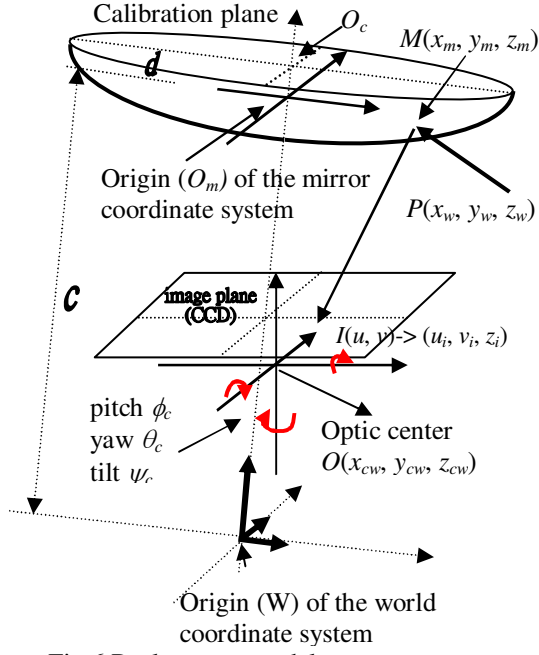


Fig.6 Real camera model.

#### 4.1 Unit Normal Vector $\vec{n}$

The unit normal vector at point  $(x_m, y_m, z_m)$  is:

$$\vec{n} = [\sin\delta \cos\varphi, \sin\delta \sin\varphi, -\cos\delta]^T.$$

Where:

$$\varphi = \tan^{-1} \frac{y_m}{x_m} \quad (14)$$

$$\sin\delta = \frac{br_m}{\sqrt{a^4 + c^2 r_m^2}}, \quad \cos\delta = \frac{a\sqrt{a^2 + r_m^2}}{\sqrt{a^4 + c^2 r_m^2}} \quad (15)$$

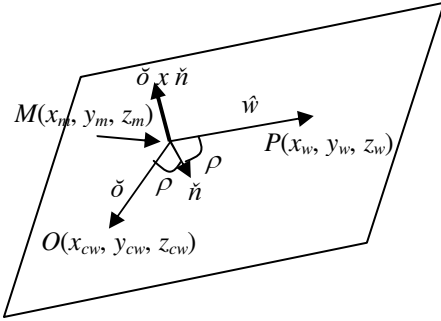


Fig.7 Co-planar vectors and cross product.

#### 4.2 Co-Planar Constraint

The points  $O(x_{cw}, y_{cw}, z_{cw})$ ,  $P(x_w, y_w, z_w)$ ,  $M(x_m, y_m, z_m)$  and normal vector  $\vec{n}$  should fit the co-planar constraint, Fig.7 shows this case.

Where,

$$MP = \vec{w} = [(x_w - x_m), (y_w - y_m), (z_w - z_m)]^T,$$

$$MO = \vec{o} = [(x_{cw} - x_m), (y_{cw} - y_m), (z_{cw} - z_m)]^T$$

The co-planar constraint holds for:

$$(\vec{o} \times \vec{n}) \cdot \vec{w} = 0 \Rightarrow$$

$$\begin{vmatrix} i & j & k \\ (x_{cw} - x_m) & (y_{cw} - y_m) & (z_{cw} - z_m) \\ \sin\delta \cos\varphi & \sin\delta \sin\varphi & -\cos\delta \end{vmatrix} \cdot \begin{pmatrix} (x_w - x_m) \\ (y_w - y_m) \\ (z_w - z_m) \end{pmatrix} = 0 \quad (16)$$

Set

$$K_{m1} = (y_m - y_{cw}) \cos\delta + (z_m - z_{cw}) \sin\delta \sin\varphi, \quad (17)$$

$$K_{m2} = (x_m - x_{cw}) \cos\delta + (z_m - z_{cw}) \sin\delta \cos\varphi, \quad (18)$$

$$K_{m3} = (x_{cw} - x_m) \sin\delta \sin\varphi - (y_{cw} - y_m) \sin\delta \cos\varphi \quad (19)$$

$$x_n = (x_w - x_m), \quad y_n = (y_w - y_m), \quad z_n = (z_w - z_m) \quad (20)$$

We get

$$K_{m1}x_n - K_{m2}y_n + K_{m3}z_n = 0 \quad (21)$$

#### 4.3 Reflection Law of Mirror

Refer to Fig.7, the angle  $\rho$  between  $MP$  and  $\vec{n}$  is equal to the angle  $\rho$  between  $MO$  and  $\vec{n}$ . The reflection law holds for

$$\cos\rho = \frac{MP \cdot \vec{n}}{\|MP\| \|\vec{n}\|} = \frac{MO \cdot \vec{n}}{\|MO\| \|\vec{n}\|} \quad (22)$$

$$\Rightarrow \cos\rho = \frac{\vec{w} \cdot \vec{n}}{\|\vec{w}\| \|\vec{n}\|} = \frac{\vec{o} \cdot \vec{n}}{\|\vec{o}\| \|\vec{n}\|}$$

Assume the unit vector of  $\vec{w}$  is

$$\vec{w}_u = \frac{\vec{w}}{\|\vec{w}\|} = [w_x, w_y, w_z]^T$$

Where

$$w_i = \frac{(i_w - i_m)}{\sqrt{(x_w - x_m)^2 + (y_w - y_m)^2 + (z_w - z_m)^2}} \quad (22-1)$$

$$= \frac{i_n}{\sqrt{x_n^2 + y_n^2 + z_n^2}}, \quad i = x, y, z$$

So, Equation (22) becomes:

$$w_x \sin\delta \cos\varphi + w_y \sin\delta \sin\varphi - w_z \cos\delta = \cos\rho \quad (23)$$

#### 4.4 Calculating Unit Vector $(w_x, w_y, w_z)$

If  $(x_n, y_n, z_n)$  is not equal  $(0, 0, 0)$ , Equation (21) also hold for

$$K_{m1} \frac{x_n}{\sqrt{x_n^2 + y_n^2 + z_n^2}} - K_{m2} \frac{y_n}{\sqrt{x_n^2 + y_n^2 + z_n^2}} + K_{m3} \frac{z_n}{\sqrt{x_n^2 + y_n^2 + z_n^2}} = 0$$

that is

$$K_{m1}w_x - K_{m2}w_y + K_{m3}w_z = 0 \quad (24)$$

The norm of the unit vector should be equal 1, so

$$w_x^2 + w_y^2 + w_z^2 = 1 \quad (25)$$

Using Equations (23), (24) and (25), we can solve the three unknown  $w_x$ ,  $w_y$  and  $w_z$ .

Set

$$A_m = \frac{\cos\delta K_{m1} + \sin\delta \cos\varphi K_{m3}}{\cos\delta K_{m2} - \sin\delta \sin\varphi K_{m3}}, \quad (26-1)$$

$$B_m = \frac{-\cos\rho K_{m3}}{\cos\delta K_{m2} - \sin\delta \sin\varphi K_{m3}}$$

We get

$$w_y = A_m w_x + B_m \quad (26-2)$$

Set

$$C_m = \frac{\sin \delta (\sin \phi K_{m1} + \cos \phi K_{m2})}{\cos \delta K_{m2} - \sin \delta \sin \phi K_{m3}}, \quad (26-3)$$

$$D_m = \frac{-\cos \phi K_{m2}}{\cos \delta K_{m2} - \sin \delta \sin \phi K_{m3}}$$

We get

$$w_z = C_m w_x + D_m \quad (26-4)$$

Equation (25) and (26-1) to (26-4) can use to solve the unit vector  $(w_x, w_y, w_z)$ .

#### 4.5 Relation between $(u, v)$ and $(x_m, y_m, z_m)$

The coordinate of point  $I$  in the camera coordinate system is  $(u, v, f)$ . So, the point  $I (u_i, v_i, z_i)$  in the mirror coordinate system can be calculated by Equation (13).

Because that the points  $O, I,$  and  $M$  lay on the same line. (See Fig. 6)

$$\tan \phi = \frac{v_i - y_{cw}}{u_i - x_{cw}} = \frac{y_m - y_{cw}}{x_m - x_{cw}} \quad (27)$$

Equation (27) can be rewritten as:

$$y_m = y_{cw} - x_{cw} \tan \phi + x_m \tan \phi \quad (27-1)$$

Set

$$K_1 = y_{cw} - x_{cw} \tan \phi \quad (28-1)$$

$$K_2 = \frac{(z_i - z_{cw})}{u_i - x_{cw}} \quad (28-2)$$

$$K_3 = z_{cw} + c - x_{cw} K_2 \quad (28-3)$$

$$K_4 = b^2 (1 + \tan^2 \phi) - a^2 K_2^2 \quad (28-4)$$

$$K_5 = b^2 K_1 \tan \phi - a^2 K_2 K_3 \quad (28-5)$$

$$K_6 = a^2 b^2 + b^2 K_1^2 - a^2 K_3^2 \quad (28-6)$$

We get

$$x_m = \frac{-K_5 \pm \sqrt{K_5^2 - K_4 K_6}}{K_4} \quad (28)$$

Using (27) and (28), we can get  $y_m$ .

Using Equation (7), we can get  $z_m$ .

## 5. Experimental Results

### 5.1 Unwarping of Simulation Scene to Perspective View

#### 5.1.1 Warping of a pseudo target to omnidirectional image

We use the real calibration data obtained in section 3.3.3, which are translation  $T(-2.99, 0.96, 88.67)$  (the unit is mm) ; rotation  $R(0.013, 0.035, 0.007)$  (the unit is radian); kappa  $\kappa_7=0.0$ ; and focal length  $f=2.9$  mm, and the mapping equations obtained in section 4 to wrap a pseudo target depicted as Fig.8 to a hypercatadioptric omnidirectional image. The target has a grid map with  $1.0 \times 1.0$  m<sup>2</sup> grid and  $20.0 \times 20.0$  m<sup>2</sup> map size. A L-shape wall with  $1.0$  m height and  $2.8$  m width in

each side is placed near the center of the grid map.

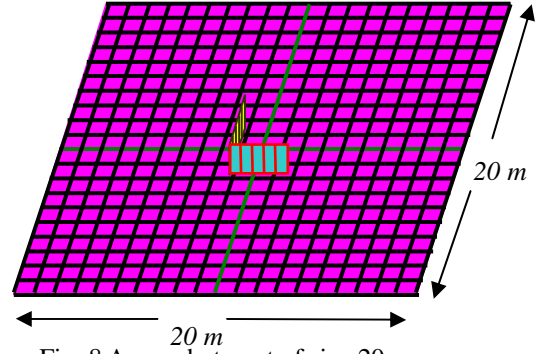


Fig. 8 A pseudo target of size 20 m x 20 m, with a L-shape wall at center position.

The target is put under our hypercatadioptric camera and the z-axis of the target coordinate system and the mirror coordinate system are aligned. The z-axis distance of the center of the target and the center of the mirror is 2.0 m. The warping picture is a  $640 \times 480$  pixel<sup>2</sup> image as Fig.9.

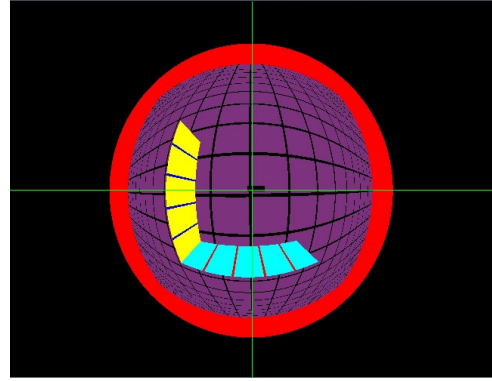


Fig.9 The warping image of the pseudo target in Fig.8.

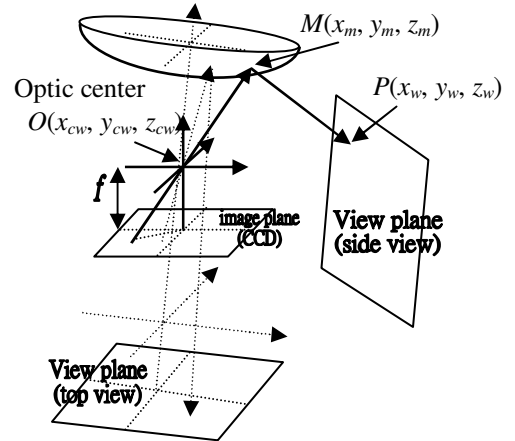


Fig.10 View planes for viewing the perspective unwarping image in the real world.

#### 5.1.2 Results of unwarping the pseudo image

To test the correctness of our derived equations, we set two kinds of view planes as Fig.10 depicts;

each one is a rectangle region, to capture the unwarping (back-projection) rays emanating from the image plane. The rectangle region is divided into  $m \times n$  (for example,  $320 \times 240$  for side view) units representing a  $m \times n$  pixel<sup>2</sup> image of perspective view of the warped target image.

Fig. 10 shows examples of the view plane setting. The top view region is set as a  $4.0 \times 4.0$  m<sup>2</sup> region lying on the x-y plane and the z-axis is aligned to the z-axis of the mirror coordinate system with 2.0 m below the origin of the mirror coordinate system. Fig.11 (a), (b), and (c) are the unwarping results with different settings for testing the correctness of our derived equations in this paper. We can see in Fig.11 (a) that our derived equations are perfectly recovering the warping image in Fig. 12 within the setting view plane region if the camera is calibrated. Fig.11 (b) and (c) tell us that insufficient calibration of the hypercatadioptric camera will suffer distorted unwarping image. Fig.11 (d), (e), and (f) are the unwarping results with assumption that the camera is a perfect designed single-viewpoint system. And so, equation (5) is used to unwarped the target image. The real sensor size should be  $3.2 \times 2.4$  mm<sup>2</sup> and the unwarping image is as Fig.11 (d). But, we can see in Fig.11 (d) that the unwarping region is really small! So, for comparison reasons, we set other sensor size as Fig.11 (e) and (f) to observe the results. Note that the setting of Fig.11 (e) and (f) are unreasonable for a real CCD sensor.

Fig.12 shows examples of a side view setting. The side view region is set with  $0.5\pi$  degree view direction at the x-y plane with center distance  $2.0/\sqrt{2}$  m apart from the z-axis of the mirror coordinate system and the z-axis range from 0 to -2.0m with

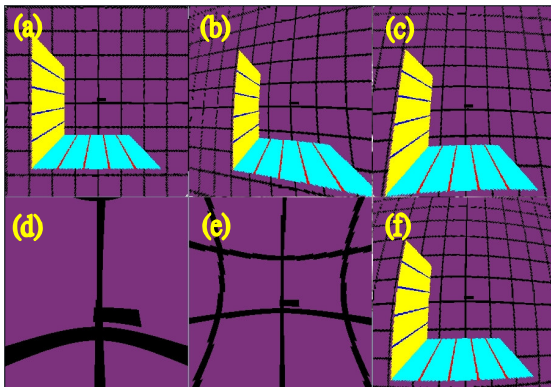


Fig.11 Unwarping image of Fig. 9 (Top view)

- (a),(b),(c) are results using equations derived from this paper with different T ( $T_x, T_y, T_z$ ) and R ( $R_x, R_y, R_z$ ) setting. Here, (a) has the same T and R as Fig. 9 used. In (b), we set  $R_x=R_y=R_z=0$ . In (c), we further set  $T_x=T_y=0$  (assume perfect alignment).
- (d),(e),(f) are results using equation (5), with different CCD sensor size. Here, an ideal single-viewpoint designed hypercatadioptric camera is assumed. In (d), sensor size is  $3.2 \times 2.4$  mm<sup>2</sup>, (e) is  $1.6 \times 1.2$  mm<sup>2</sup>, and (f) is  $0.8 \times 0.6$  mm<sup>2</sup>.

respect to the origin of the mirror coordinate system. Fig.12 (a) to (d) are the four directional views with our derived equations. Fig.12 (e) and (f) are the same directional view with (b) and (c), but with SVP equation (5). It can be seen that the vertical lines are tilted in Fig.12 (e) and (f).

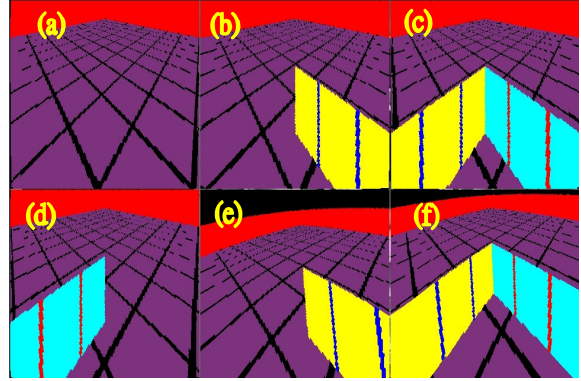


Fig. 12 Unwarping image of Fig. 9 (Side view)

- (a),(b),(c),(d) are results using equations derived from this paper with the same T and R as Fig.9 used. Here, (a) is viewing from  $1.5\pi$  to  $2.0\pi$ , (b) is viewing from  $1.0\pi$  to  $1.5\pi$ , (c) is viewing from  $0.5\pi$  to  $1.0\pi$ , and (d) is viewing from  $0.0\pi$  to  $0.5\pi$ .
- (e),(f) are results using equation (5) with different viewing angle. (e) is the same as (b), (f) is the same as (c). Here, an ideal single viewpoint designed hypercatadioptric camera is assumed. In (e) and (f), the sensor size is  $0.8 \times 0.6$  mm<sup>2</sup>.

## 5.2 Unwarping of Real Scene to Perspective View

Fig.13 and Fig.14 are the Unwarping results of real image (Fig.4) taken by the calibrated camera in this paper. The parameter settings of Fig.13 and Fig.14 are the same as Fig.11 and Fig.12, except that the pseudo simulated warping image is replaced by the real image of Fig.4. We observe that the unwarping results of Fig.13 (a) and Fig.14 (a) are not as best as the simulation pseudo scenes in Fig.11 (a) and Fig.12 (a). Two reasons can interpret these results: (1) there are residual errors after camera calibration, (2) the “external” calibration between the mirror coordinate system (used in this paper as the world coordinate system) and the real world (for example: the room) coordinate system has not been done. We believe that if using precise calibration pattern created at the same time that the hypercatadioptric camera is manufactured to replace the experimental paper-made pattern in this paper, the residual errors of calibration will be reduced. The problem caused by (2) is not serious; it can be removed using traditional calibration. If we carefully align the parallelism of the mirror plane with the floor of the room, the problem caused by (2) almost can be ignored.

## 6. Conclusions

In this paper, the image unwarping of the non



single-viewpoint hypercatadioptric camera is studied. We use the calibration information to derive the precise unwarping equations for the hypercatadioptric camera no matter it is SVP designed or not. The derived equations are validated to have the same performance as a perfectly designed SVP camera when deducing the calibration parameters to fit the SVP constraints. Furthermore, we show the benefits of our method beyond the SVP method with a little deviation from the SVP constraints by setting  $R_x$  one degree rotated. From the simulated results, we confirm the correctness of our method.

#### References:

- [1] S. Nayar, "Catadioptric Omnidirectional Camera," *IEEE Conf. Computer Vision and Pattern Recognition*, pp. 482-488, June 1997.
- [2] Rahul Swaminathan, Michael D. Grossberg and Shree K. Nayar, "Caustics of Catadioptric Cameras," *Computer Vision, 2001. ICCV 2001. Proceedings*, Eighth IEEE International Conference on , Volume: 2 , 2001, Page(s): 2 -9 vol.2.
- [3] Kazumasa YAMAZAWA, Yasushi YAGI and Masahiko YACHIDA, "Omni directional Imaging with Hyperboloidal Projection," *Proceedings of the 1993 IEEE/RSJ International Conference on Intelligent Robots and Systems*, Yokohama, Japan July 26-30, 1993, pp. 1029-1034.
- [4] Yoshio Onoe, Naokazu Yokoya, Kazumasa Yamazawa, and Haruo Takemura, "Visual Surveillance and Monitoring System Using an Omnidirectional Video Camera," *Pattern Recognition, 1998. Proceedings*, Fourteenth International Conference on , Volume: 1 , 16-20 Aug 1998, Page(s): 588 -592 vol.1.
- [5] R. Y. Tsai, "An Efficient and Accurate Camera Calibration Technique for 3D Machine Vision," *Proc. IEEE Conference on Computer Vision and Pattern Recognition*, pp. 364-374, 1986.
- [6] Joaquim Salvi, Xavier Armangué, Joan Batle, "A Comparative review of camera calibrating methods with accuracy evaluation," *Pattern Recognition*, 35, 2002, pp.1617-1635.
- [7] Christopher Geyer and Kostas Daniilidis, "Paracatadioptric Camera Calibration," *IEEE Transactions on Pattern Analysis and Machine Intelligence*, Vol. 24, No. 5, pp.687-695, May 2000.
- [8] Christopher Geyer and Kostas Daniilidis, "Catadioptric Camera Calibration," *Proc. Seventh IEEE International Conference on Computer Vision*, Vol. 1, pp.398-404, 1999.
- [9] Sing Bing Kang, "Catadioptric self-calibration," *IEEE Conf. Computer Vision and Pattern Recognition*, pp.201-207, June 2000.
- [10] Daniel G. Aliaga, "Accurate Catadioptric Calibration for Real-time Pose Estimation in Room-size Environments," *Proc. Eighth IEEE*

*International Conference on Computer Vision*, Vol. 1, pp.127-134, 2001.

- [11] Jonathan Fabrizio, Jean-Philippe Tarel and Ryad Benosman, "Calibration of Panoramic Catadioptric Sensors Made Easier," *Proc. Third Workshop on Omni directional Vision*, IEEE 2002.

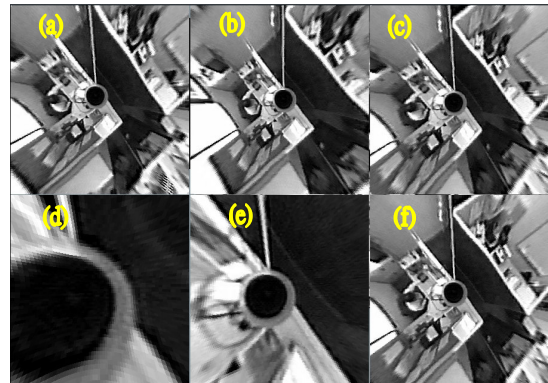


Fig. 13 Unwarping image of real scene Fig. 4 (Top view)

- (a),(b),(c) are results using equations derived from this paper with different  $T (T_x, T_y, T_z)$  and  $R (R_x, R_y, R_z)$  setting. Here, (a) has the same  $T$  and  $R$  as Fig. 9 used. In (b), we set  $R_x=R_y=R_z=0$ . In (c), we further set  $T_x=T_y=0$ (perfect alignment).
- (d),(e),(f) are results using equation (5), with different CCD sensor size. Here, an ideal single viewpoint designed hypercatadioptric camera is assumed. In (d), sensor size is  $3.2 \times 2.4 \text{ mm}^2$ , (e) is  $1.6 \times 1.2 \text{ mm}^2$ , and (f) is  $0.8 \times 0.6 \text{ mm}^2$ .



Fig. 14 Unwarping image of real scene Fig.4 (Side view)

- (a),(b),(c),(d) are results using equations derived from this paper with the same  $T$  and  $R$  as Fig. 9 used. Here, (a) is viewing from  $1.5\pi$  to  $2.0\pi$ , (b) is viewing from  $1.0\pi$  to  $1.5\pi$ , (c) is viewing from  $0.5\pi$  to  $1.0\pi$ , and (d) is viewing from  $0.0\pi$  to  $0.5\pi$ .
- (e),(f) are results using equation (5) with different viewing angle. (e) is the same as (b), (f) is the same as (c). Here, an ideal single viewpoint designed hypercatadioptric camera is assumed. In (e) and (f), the sensor size is  $0.8 \times 0.6 \text{ mm}^2$ .